Modelling the compression and reorganization of cell aggregates

Vol. , No. , 2011, pp.

Modelling the compression and reorganization of cell aggregates

C. Giverso[1] *, **L. Preziosi**[1]

[1] Department of Mathematics, Politecnico di Torino, Corso Duca degli Abruzzi 24, 10129 Torino, Italy

Abstract.

In this paper we study the mechanical behavior of multicellular aggregates using the notion of multiple natural configurations. In particular, we extend the elasto-visco-plastic model proposed in [18] taking into account of the liquid constituent present in cellular spheroids. Aggregates are treated as porous materials, composed of cells and filled with water. The cellular constituent is responsible for the elastic and the plastic behavior of the material. The plastic component is due to the rearrangement of adhesion bonds between cells is translated into the existence of a yield stress in the macroscopic constitutive equation. On the other hand, the liquid constituent is responsible of the viscous-like response during deformation. The general framework is then applied to describe the uniaxial homogeneous compression both when a constant load is applied and when a fixed deformation is imposed and subsequently released. We compare the results of the model with the dynamics observed during the experiments in [10].

Key words: aggregate compression, living tissues rheology, elasto-visco-plasticity

1. Introduction

Cells and biological tissues are complex materials, made of multiple subelements [29]: each cell is bounded by the plasma membrane to form a closed object containing the nucleus and a fluid, the cytosol (made of water, soluble proteins, sugar and salt), where numerous organelles are immersed. An important intracellular structure, that plays a key role in many biological process (e.g. maintaining cell shape, enabling movement, aiding cellular division) and that strongly affects cell mechanical behavior, is the cytoskeleton, a complex meshwork of polymers crossing through the cytosol. Each subcellular element is different from the other and mechanical properties are non-

*Corresponding author. E-mail: chiara.giverso@polito.it

homogenously localized inside each of them [31]. For instance, cytoplasm properties strongly depend on the amount of actin or tubulin and on the degree of polymerisation of these filaments. Similarly, the membrane has a bending modulus which is dependent on proteins embedded into it [31]. This high heterogeneity in cell composition and in subcellular properties makes mechanical response difficult to be modelled even for a single cell. In addition, cellular materials are different from usual soft materials because they can develop an active response when submitted to stresses. This response is due to mechanotransduction, which is the ability of cells to transform mechanical external stresses into biochemical signals (and vice versa) in order to transfer information to and from the nucleus [6, 17, 31]. This ability of cells to deform and generate forces in an active manner, coupled with their extreme complexity and their non linear response to mechanical stimuli outlines the need of a specific mathematical model to describe cellular dynamics.

Furthermore, cells are able to interact with each other to form tissues and multicellular aggregates in some stages of their life. The rheological properties of such materials are quite uncommon, because they contain both cells and fluids embedded inside each cell and in the extracellular matrix (ECM) among them. It is then known that not only the intrinsic properties of the base components - cells and collagen - but also their relative concentration can affect the rheological properties of multicellular aggregates [7, 8, 30, 31].

Therefore there are big theoretical difficulties in considering a cell aggregate as a liquid or as a solid. Indeed, treating it like a fluid may bring some simplifications (e.g. to deal with velocities rather than deformations). However, the fact that the cellular liquid is contained in a solid structure, puts in evidence the simplifications introduced by such an hypothesis. On the other hand, it is not correct to consider multicellular spheroids as elastic solids, because they are composed of living material: cells forming the aggregates continuously duplicate and die, the ECM is constantly remodelled by the same cells and, even in absence of growth and death, cells can reorganize in response to an external mechanical stimulus. Therefore it is impossible to define a fixed natural.

Due to this complexity, the mechanical behavior of multicellular systems is still far from being understood and most of our knowledge concerning the rheological and mechanical properties of cell aggregates comes from previous studies on soft biological tissues [30, 31], usually corresponding to visco-elastic materials or to non-Newtonian fluids [13]. However, cellular aggregates have been shown to play an important role in many biological phenomena and it has been recently found that many pathologies are characterized by an alteration of cell mechanical behaviors and hence the response of soft biological tissues may serve as an important diagnostic parameter in the early detection of diseases [16, 25] and in the diagnosis of tumor metastatic potential [32]. Therefore a more detailed description of aggregates mechanical properties is needed. Indeed, in the recent years there have been many studies focused on cell microrheology and mechanical behavior, aimed both at establishing the constitutive equation of cells and aggregates [1, 2, 3, 18] and at measuring properties like cell interfacial energy, elastic modulus and relaxation times [10, 11, 12, 32]. In particular, in [3, 18] it was shown that the phenomena observed during some compression experiments performed in [10, 11, 12], where a fixed deformation is applied to the cell aggregate, or in [15], where a dense cell suspension is subjected to shear, can be explained using the concept that the natural configuration evolves, due to the rearrangement of adhesion bonds. Then, aggregate mechanical behavior can be modelled coupling the viscoelastic behaviors with a yield condition,

generating a plastic reorganization, when the stress becomes too high.

However, pressure controlled experiments (e.g. creep test) can not be fully explained with the models in [3, 18]. Indeed experimental evidences [10, 11, 12] suggest that, when an imposed deformation is removed, the shape recovery dynamics of aggregates, requires some times. On the contrary in [1, 2, 3, 18, 19], when the stress is released, the shape recovery is instantaneous. A similar behavior is found when a stress is suddenly applied. In addition, if the stress imposed is sufficiently high, the initial configuration is no more reached, which can not be described in the models presented in [10, 11, 12], that are based essentially on the existence of a surface tension holding together the cell aggregate. A similar difficulty is encountered when dealing with the description of periodic compressions of the spheroid.

The purpose of this work is then to extend the elasto-visco-plastic model in [18] to include the effects described above. On one hand, we take into account of the existence of a maximum stress that can be sustained by the cell aggregate before reorganizing and on the other hand, we consider the fact that the total stress exerted by the specimen is not only due to the cellular component, but also to a further viscous term due to the action of the liquid phase.

The structure of the paper is the following: after introducing the constitutive equation in Section 2, the model is applied to cell aggregate compression and release in Section 3. In Section 4, the constitutive model is used to simulate the behavior of cellular spheroids under compression at constant load, possibly repeated over time (Section 4.1) and under a cycle of constant deformation and stress releases, as in [10] (Section 4.2). The results obtained with the model (in terms of spheroid deformation and applied stress) are compared with the prediction of previous models [18, 19] and mechanical experiments performed in [10]. The qualitative properties of the solution are described in detail, with proofs reported in the Appendix.

2. The Constitutive Model of Cell Aggregates

Cellular spheroids used in biological experiments [10, 11, 12] have a diameter ranging from 200 and 600 μm, which means a number of cells between ten and two hundred thousand. Therefore cell aggregates can be modelled as continuum media, presenting elastic, viscous and plastic behaviors:

- the elastic component is mainly due to the cytoskeleton, which is composed of elastic filaments strongly cross-linked,
- the dissipative component, responsible of the viscous behavior, originates primarily from the flow of the cytosol along with and through the cytoskeleton meshwork and from extracellular fluid movements,
- the plastic component is due to the re-organization of adhesion bonds between cells and to actin network remodelling inside cells.

Hence, a mathematical model aiming at capturing cell aggregate mechanics has to consider all these properties. The main difficulty in describing cell aggregates and biological tissues consists

in the fact that even in the absence of growth the ensemble of cells undergoes an internal re-organization in response to an applied strain or stress, which is macroscopically translated in plastic deformation.

Addressing this problem, Ambrosi and Mollica [1, 2], proposed to investigate cell aggregate mechanics with the aid of the theory for materials with evolving natural configurations. This setting, introduced in [20, 21, 22, 27], has been successfully applied to describe the growth and remodelling of several tissues, allowing to model separately the contribution due to growth from the one due to deformation alone (see [4] for a review). The total evolution of the tissue is given through the deformation tensor $\mathbf{F}$, which is a mapping from the tangent space related to the initial (or reference) configuration, $\mathcal{K}_0$, onto the tangent space related to the current configuration $\mathcal{K}_c$ and represents how the body is deforming locally. Then it is possible to consider the map from $\mathcal{K}_0$ to $\mathcal{K}_c$ as composed of three parts: the first one related to pure growth/death (therefore accompanied with mass variation, here neglected), the second one due to internal rearrangement of cells and the third one due to stress-induced deformation (both without change of mass). This consideration leads to the introduction of two virtual configurations: the "grown configuration", $\mathcal{K}_p$ that represents cells that have undergone pure growth, without undergoing either remodelling or stress-induced deformation and the natural (or locally stress-free) state $\mathcal{K}_n$, which takes into account cell internal re-organization [3, 18].

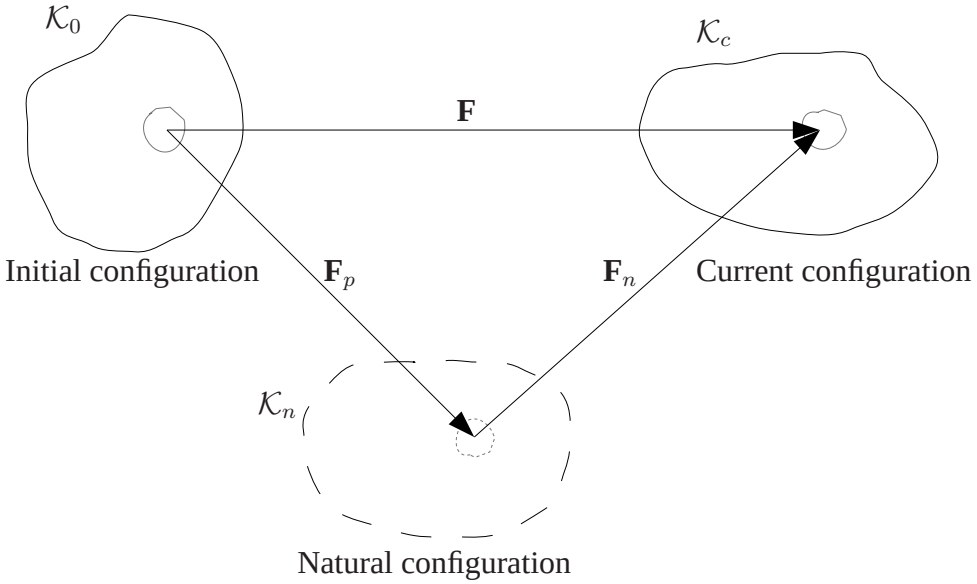

Figure 1: Diagram of the states from the original unstressed configuration $\mathcal{K}_0$ to the current configuration $\mathcal{K}_c$, in the framework of multiple natural configurations. $\mathcal{K}_n$ represents the natural state, which takes into account cell internal re-organization.

In particular, in the case of mechanical testing of multicellular aggregates, it is natural to assume that no growth occurs during stress-induced deformation, since mitosis and apoptosis occur on a much longer time scale (several hours) than the typical time scale of mechanical deformation. Therefore, referring to Figure 1, one can introduce the following multiplicative decomposition of the deformation gradient

$$\mathbf{F} = \mathbf{F}_n \mathbf{F}_p \,, \tag{2.1}$$

where $\mathbf{F}_n$ identifies the deformation without cell re-organization (describing how the body is deforming locally while going from the natural configuration $\mathcal{K}_n$ to $\mathcal{K}_c$), $\mathbf{F}_p$ describes the internal re-organization of cells (evolution from $\mathcal{K}_0$ to $\mathcal{K}_n$).

Cell and aggregate responses to mechanical stimuli have been successfully described using this framework in [3, 18, 19]. However, the viscous contribution of the liquid encapsulated inside the multicellular system has always been neglected.

The aim of this work is to describe cell aggregate mechanics using the concept of materials with evolving natural configuration, treating the system as a deformable porous material filled with physiological liquid.

The volume ratio of the solid phase is denoted by ϕ_c, the liquid one by ϕ_ℓ and obviously the saturation assumption holds: $\phi_c + \phi_\ell = 1$. Then the total tension of the mixture as a whole, $\mathbf{T}_m$, is due both to the stress exerted by the cellular constituent, $\mathbf{T}_c$, and to the one exerted by the fluid contained in the cells and in which the spheroid is immersed, $\mathbf{T}_\ell$

$$\mathbf{T}_m = \phi_c \mathbf{T}_c + \phi_\ell \mathbf{T}_\ell = \phi_c \mathbf{T}_c + (1 - \phi_c)\mathbf{T}_\ell \,. \tag{2.2}$$

Treating the fluid as a linear incompressible Navier-Stokes fluid and assuming that cells and liquid move with the same velocity, the second term in equation (2.2) reads $\mathbf{T}_\ell = -p\mathbf{I} + 2\nu\mathbf{D}$, where $\mathbf{D} = \frac{1}{2}(\mathbf{L} + \mathbf{L}^T)$ is the symmetric part of velocity gradient, $\mathbf{L} = \dot{\mathbf{F}}\mathbf{F}^{-1}$, whereas p is a Lagrangian multiplier due to the volume additivity of the constituents and it represents the interstitial fluid pressure that will also appear in the stress tensor for the cellular constituent.

Obviously this is only an approximation and a better description of the phenomenon should take into account of the porous structure and the relative motion of the liquid with respect to cells as given, for instance, by Darcy's law. The introduction of the viscous term is consistent with Saramito's work [23, 24] on elasto-visco-plastic fluids, such as liquid foams, emulsions and blood flows. Indeed in these works the 1D total stress is represented by $\sigma = \tau + \eta\dot{\varepsilon}$, where τ is an extension of the Oldroyd model coupled with the Bingham constitutive equation, whereas the second term takes into account of viscous phenomena.

It is important to observe that, in (2.2), the viscous coefficient, ν, is proportional to the viscosity of the fluid encapsulated in the cellular specimen, but it is not simply the viscosity of the physiological liquid. As explained in Section 3, an estimate for this coefficient can be derived

linking the consolidation time of a porous medium filled with liquid to the characteristic time of the model presented in this paper.

Concerning the tensor $\mathbf{T}_c$ representing the response of the cellular constituent, we refer to [18], where elasto-visco-plastic effects are included starting from the idea that the rearrangement of adhesion bonds during the deformation of multicellular spheroids is related to the existence of a yield condition in the macroscopic constitutive equation of the stress tensor. The yield stress is a very important quantity in rheology and it is associated with the existence of strong interactions, causing the impossibility for a fluid to flow when small shear stresses are applied.
Indeed experimental evidences suggest that when a cell aggregate undergoes compression:

1. for moderate values of applied stress, cell aggregates deform elastically;

2. above a limit value, the cell aggregate undergoes internal re-organization which can be modelled at a macroscopic level as a visco-plastic deformation.

The so-called yield stress, denoted by $\tau(\phi_c)$, depends on the number of cells per unit volume because the threshold of the onset of cell re-organization is proportional to the area of the cell membranes in contact times the bond energy, that represents the work needed to break cell-to-cell bonds. This is related to the experimental observation that adhesion bonds between cells have a finite strength and might break or build up during the evolution [5, 9, 26].

To translate this idea into formal terms, we propose a modification of the model presented in [18]. Using the virtual-power formulation and considering that the Cauchy tensor, $\mathbf{T}_c$, is workconjugate with the elastic deformation rate $\mathbf{L}_n = \dot{\mathbf{F}}_n\mathbf{F}_n^{-1}$ whereas the plastic tensor, $\mathbf{T}_p$, is workconjugate with $\mathbf{L}_p = \dot{\mathbf{F}}_p\mathbf{F}_p^{-1}$, it can be proved [14] that

$$\mathbf{T}_p = J\mathbf{F}_n^T\mathbf{T'}_c\mathbf{F}_n^{-T}\,, \tag{2.3}$$

where $\mathbf{T'}_c = \mathbf{T}_c - \frac{1}{3}(tr\mathbf{T}_c)\mathbf{I}$ is the deviatoric part of $\mathbf{T}_c$.

Introducing a constitutive free energy ψ and postulating a dissipation principle, the following inequality holds

$$\dot{\psi} - \mathbf{T}_c \cdot \mathbf{L}_n - \mathbf{T}_p \cdot \mathbf{L}_p \leq 0\,. \tag{2.4}$$

Then taking $\psi = \hat{\psi}(\mathbf{F}_n)$ and using the classical Coleman-Noll procedure for the exploitation of second law of thermodynamics, we obtain

$$\mathbf{T}_c = \frac{\partial\hat{\psi}}{\partial\mathbf{F}_n}\mathbf{F}_n^T \tag{2.5}$$

$$\mathbf{T}_p \cdot \mathbf{L}_p \geq 0\,. \tag{2.6}$$

Therefore $\mathbf{L}_p = G\mathbf{T}_p$ satisfies the previous relations, given any positive linear functional G on the natural configuration space.

Taking into account the mechanical observations on the existence of a yield criterion and the fact that the material can be considered isotropic, we can choose

$$G = \frac{\phi_c}{2\eta(\phi_c)} \left[1 - \left(\frac{\tau(\phi_c)}{f(\mathbf{T'}_c)} \right)^{\alpha} \right]_+ sym() \,, \tag{2.7}$$

where $f(\phi_c \mathbf{T'}_c)$ is a suitable frame invariant measure of the stress of the cellular constituent, $[]_+$ and sym respectively stand for the positive and the symmetric part of their arguments. The parameter α is in the range $[0, 1]$ and determines the viscous behavior at high shear rates. In the following, the particular case $\alpha = 1$ will be considered, to obtain the following constitutive equation

$$\mathbf{L}_p = \mathbf{D}_p = \frac{\phi_c}{2\eta(\phi_c)} \left[1 - \frac{\tau(\phi_c)}{f(\mathbf{T'}_c)} \right]_+ sym \left(\mathbf{F}_n^T \mathbf{T'}_c \mathbf{F}_n^{-T} \right) \,, \tag{2.8}$$

assuming isochoric transformations, $J = 1$.
Equation (2.8) can be interpreted, considering that a crucial role in the reorganization of cells is played by the shear $\mathbf{t} \cdot \mathbf{T'}_c \mathbf{n}$ that can be mapped back to the natural configuration taking into account that a material vector transforms like $\mathbf{t} = \mathbf{F}_n \mathbf{t}_n$ whereas the normal to a material surface like $\mathbf{n} = det(\mathbf{F}_n) \mathbf{F}_n^{-T} \mathbf{n}_n = \mathbf{F}_n^{-T} \mathbf{n}_n$, since $\mathbf{F}_n$ is an isochoric transformation. Then, one has that $\mathbf{t} \cdot \mathbf{T'}_c \mathbf{n} = \mathbf{t}_n \cdot \mathbf{F}_n^T \mathbf{T'}_c \mathbf{F}_n^{-T} \mathbf{n}_n$. Therefore a crucial role in determining whether the material reorganizes is the tensor $\mathbf{T}_p = \mathbf{F}_n^T \mathbf{T'}_c \mathbf{F}_n^{-T}$.
Referring back to equation (2.8), we explicitly observe that

$$tr(\mathbf{T'}_c) = tr(\mathbf{F}_n^T \mathbf{T'}_c \mathbf{F}_n^{-T}) = tr(\mathbf{D_p}) = 0, \tag{2.9}$$

and that the eigenvalues of $\mathbf{F}_n^{-T} \mathbf{T'}_c \mathbf{F}_n^T$ are the same as those of $\mathbf{D}_p$.
Furthermore being $\mathbf{T'}_c$ objective, we have to study how the quantities in equation (2.8) transform under an euclidean change of frame. Denoting with a star $(^*)$ the value of a field after the change of frame and with $\mathbf{Q}$ an orthogonal tensor, thanks to the following relations

$$\mathbf{F}_n^* = \mathbf{Q} \mathbf{F}_n \tag{2.10}$$

$$\mathbf{F}_p^* = \mathbf{F}_p \,, \tag{2.11}$$

one has

$$\mathbf{D}_p = \mathbf{D}_p^* = G(\mathbf{F}_n^T \mathbf{T'}_c \mathbf{F}_n^{-T})^* = G \mathbf{F}_n^T \mathbf{Q}^T \mathbf{T'}_c^* \mathbf{Q} \mathbf{F}_n^{-T} \,, \tag{2.12}$$

which implies the frame indifference of $\mathbf{T'}_c$.

We remark that in the limit of small deformation with respect to the natural configuration, i.e. $|\mathbf{B}_n \cdot \mathbf{I} - 3| \ll 1$, equation (2.8) simplifies in $\mathbf{D}_p = G \mathbf{T'}_c$, that is the relation sometimes given in plasticity theory, assuming $\mathbf{F}_n$ sufficiently small. Moreover the proposed constitutive model, in the case of $\alpha = 1$ simplifies in

$$\dot{\mathbf{T}}'_c + \frac{1}{\lambda} \left[1 - \frac{\tau(\phi_c)}{f(\phi_c \mathbf{T'}_c)} \right]_+ \mathbf{T'}_c = 2\mu \left(\mathbf{D} - \frac{1}{3} (tr\mathbf{D}) \mathbf{I} \right) \tag{2.13}$$

where $\lambda = \dfrac{\eta(\phi_c)}{\mu\phi_c}$ is the *cell-reorganization time* (or plastic rearrangement time). We observe that in (2.13), the term containing the yield stress plays the role of a stress relaxation term but it switches on just when the stress overcomes the yield stress in terms of the set measure. In this case the energy is no longer elastically stored but it is spent in cell unbinding and cytoskeleton reorganization at the microscopic scale, which produces the spheroid rearrangement at the macroscopic scale. Otherwise, for $f(\phi_c \mathbf{T'}_c) < \tau(\phi_c)$, this equation can be integrated to give back the elastic equation, $\mathbf{T'}_c = \mu \left(\mathbf{B}_n - \dfrac{1}{3}(tr\mathbf{B}_n)\mathbf{I} \right)$.

3. Uniaxial compression

In this section we will study in more detail the response of a material satisfying (2.2) - (2.8) subject to a uniaxial compression test. Though the results of this section also apply to an elongation test, we focus on compressive forces. Typical experiments can be performed under the following conditions:

- a constant load is imposed to the specimen and the corresponding deformation is recorded upon time. Possibly the compression is released after some time allowing a stress-free evolution of the specimen. Then, the process of compression with the same constant load can be re-iterated. Usually, the first experiment is called *creep test* and for this reason, in the following, we will denote the last process as *cyclic creep test*.

- a fixed deformation is applied and the evolution of the stress inside the body is monitored (*stress relaxation test*). Finally the same deformation is applied periodically, letting spheroids to freely expand between two subsequent compressions. In the following we will refer to this process as *cyclic deformation test*.

We will assume that the deformation, generated by a uniaxial force or strain applied along the z-axis, is homogeneous inside the body, keeping a constant volume ratio ϕ_c, and is given by

$$x = \frac{X}{\sqrt{\psi(t)}}, \quad y = \frac{Y}{\sqrt{\psi(t)}}, \quad z = \psi(t) Z \, . \tag{3.1}$$

Then the deformation gradient from the initial to the final configuration is given by

$$\mathbf{F} = \text{diag} \left\{ \frac{1}{\sqrt{\psi(t)}}, \frac{1}{\sqrt{\psi(t)}}, \psi(t) \right\} \, . \tag{3.2}$$

The deformation gradient due to the internal reorganization of the cytoskeleton can be represented by

$$\mathbf{F}_p = \text{diag}\left\{\frac{1}{\sqrt{\Psi_p(t)}}, \frac{1}{\sqrt{\Psi_p(t)}}, \Psi_p(t)\right\}\ , \tag{3.3}$$

where $\Psi_p(t)$ is a measure of how much the aggregate has reorganized and the natural configuration has evolved. For $\Psi_p(t) = 1$ we have no contribution due to rearrangement of bonds inside the body.

From equations (3.2) and (3.3), being $\mathbf{F} = \mathbf{F}_n\mathbf{F}_p$ it is clear that

$$\mathbf{F}_n = \text{diag}\left\{\sqrt{\frac{\Psi_p(t)}{\psi(t)}}, \sqrt{\frac{\Psi_p(t)}{\psi(t)}}, \frac{\psi(t)}{\Psi_p(t)}\right\}\ . \tag{3.4}$$

Assuming that the cellular spheroid obeys a neo-Hookean law, the first term of the sum in equation (2.2) is

$$\mathbf{T}_c = -p\mathbf{I} - \Sigma_c(\phi_c)\mathbf{I} + \mu\mathbf{B}_n\ , \tag{3.5}$$

where $\Sigma_c(\phi_c)$ is the symmetric part of the cellular constituent stress tensor .

Therefore considering that in the uniaxial compression test, the total force is applied in the z-direction, one has

$$\mathbf{T}_m = -\left(p + \phi_c\Sigma_c(\phi_c)\right)\mathbf{I} + \mu\phi_c\mathbf{B}_n + 2(1-\phi_c)\nu\mathbf{D} = \text{diag}\left\{0, 0, -P_{appl}(t)\right\}\ , \tag{3.6}$$

where we consider P_{appl} to be positive for a compressive load.
In a creep test, P_{appl} is a known constant and it vanishes in the stress release phase, whereas it is a function of time in a stress-relaxation experiment under constant deformation.

Considering that the liquid and the cellular component move with the same velocity, $\mathbf{D} = \text{diag}\left\{-\frac{1}{2}, -\frac{1}{2}, 1\right\}\frac{\dot{\psi}(t)}{\psi(t)}$.
Then, being $\mathbf{B}_n = \text{diag}\left\{\frac{\Psi_p(t)}{\psi(t)}, \frac{\Psi_p(t)}{\psi(t)}, \frac{\psi^2(t)}{\Psi_p^2(t)}\right\}$ and denoting with $\Sigma = p + \phi_c\Sigma_c(\phi_c)$, we obtain the following equation for the stress exerted by the mixture.

$$\begin{aligned}\mathbf{T}_m \ &= \ -\Sigma\mathbf{I} + \mu\phi_c\,\text{diag}\left\{\frac{\Psi_p(t)}{\psi(t)}, \frac{\Psi_p(t)}{\psi(t)}, \frac{\psi^2(t)}{\Psi_p^2(t)}\right\} + \\ &\quad + 2\nu(1-\phi_c)\text{diag}\left\{-\frac{1}{2}, -\frac{1}{2}, 1\right\}\frac{\dot{\psi}(t)}{\psi(t)}\ ,\end{aligned} \tag{3.7}$$

or from (3.6)

$$\Sigma(t) = \mu\phi_c\frac{\Psi_p(t)}{\psi(t)} - \nu(1-\phi_c)\frac{\dot{\psi}(t)}{\psi(t)}\,, \tag{3.8}$$

$$P_{appl}(t) = \mu\phi_c\frac{\Psi_p^3(t)-\psi^3(t)}{\Psi_p^2(t)\psi(t)} - 3\nu(1-\phi_c)\frac{\dot{\psi}(t)}{\psi(t)}\,. \tag{3.9}$$

The first terms in the sum of both (3.8) and (3.9) are the same obtained in [18], taking account of the cellular constituent only, whereas the second terms arise from the introduction of the viscous phase in the model. Equation (3.9) can provide the stress exerted by the aggregate when a deformation is imposed along the z-axis (e.g. a fixed deformation, ψ_0), or it can be used to derive the evolution of $\psi(t)$ when, for instance, a constant load is applied

$$\frac{\dot{\psi}}{\psi} = -\frac{P_{appl}}{3\nu(1-\phi_c)} + \frac{\mu\phi_c}{3\nu(1-\phi_c)}\frac{\Psi_p^3-\psi^3}{\psi\Psi_p^2}\,, \tag{3.10}$$

where we omit the dependence from t for sake of simplicity. As a particular case, equation (3.10) can be used to model the stress-free evolution of the system, imposing $P_{appl} = 0$. We can observe that the ratio ν/μ represents a characteristic time in equation (3.10). Considering the fact that we are compressing a multicellular aggregate, this characteristic time can be related to the consolidation time of a saturated porous material filled with fluid, $\frac{\mu_w L^2}{kE}$, where μ_w is the dynamic viscosity of the physiological liquid, L the multicellular aggregate height, k the permeability of the porous structure and E its elastic modulus. In this way it is possible to derive the parameter ν from physical quantities measurable in experiments and by means of known estimates of k, e.g. the Kozeny-Carman relation.

Equation (3.10) need to be joined with equation (2.8), taking into account that

$$\mathbf{T}_c' = \mu\ \mathrm{diag}\left\{-\frac{1}{3}, -\frac{1}{3}, \frac{2}{3}\right\}\frac{\psi^3-\Psi_p^3}{\Psi_p^2\psi}\,. \tag{3.11}$$

and postulating an equation for $f(\phi_c\mathbf{T}_c')$.
Here we consider that the frame invariant measure of the stress is the maximum shear stress magnitude, given by half of the difference between the maximum and the minimum stress in the principal directions (Tresca's criterion)

$$f(\phi_c\mathbf{T}_c') = \frac{\mu\phi_c}{2}\frac{|\Psi_p^3-\psi^3|}{\psi\Psi_p^2}\,, \tag{3.12}$$

which means that cell unbinding is primarily caused by the slippage of cells along the maximum shear stress surface, which seems reasonable in a cellular aggregate under compression. In a more

general case, in which the principal stresses are not trivially known, it is possible to use the von Mises criterion, taking into account that Tresca's criterion is more conservative and, therefore, it predicts plastic reorganization for stresses that are still elastic according to the von Mises criterion. The evolution for the internal reorganization is therefore

$$\frac{\dot{\Psi}_p}{\Psi_p} = -\frac{1}{3\lambda}\left[1 - \frac{2\tau}{\mu\phi_c}\frac{\psi\Psi_p^2}{|\Psi_p^3 - \psi^3|}\right]_+ \frac{\Psi_p^3 - \psi^3}{\psi\Psi_p^2} \,. \tag{3.13}$$

where $\lambda = \dfrac{\eta(\phi_c)}{\mu\phi_c}$, as previously defined, and $\tau = \tau(\phi_c)$.
Equation (3.13) states that when the quantity inside the square parenthesis is positive, then Ψ_p will evolve.
Considering that $\Psi_p(0) = 1$,

$$\frac{1}{\psi} - \psi^2 > \frac{2\tau}{\mu\phi_c} \tag{3.14}$$

is called in the following *yield condition* because it determines the deformation that switches on the evolution of Ψ_p. For $\psi \in (0, 1]$, the right hand side of equation (3.14) is a positive and decreasing function of ψ and therefore only values of ψ sufficiently small, so that the yield condition is satisfied, are able to trigger the internal reorganization inside spheroids.
We observe that, as we will see more in detail in the following section, in a stress relaxation experiment with constant deformation equal to ψ_0 satisfying (3.14) the equilibrium of (3.13) is reached when $\dfrac{\Psi_p^3 - \psi_0^3}{\psi_0\Psi_p^2} = \dfrac{2\tau}{\mu\phi_c}$, i.e. from (3.10) at $P_{appl} = 2\tau$, independently of ψ_0 as in [18].

4. Results and Discussion

The model presented in Section 3 can provide some useful information on the mechanical behavior of aggregates both when they are compressed with a constant force and when they are released. In Section 4.1 we present the results obtained in the case of a cyclic creep test and then in Section 4.2 those in the case of a cyclic deformation test, as performed in the experiments in [10].
The following proposition, proved in the Appendix, will be useful.

Proposition 1. *When the aggregate is compressed according to the following imposed deformation and stress histories:*

a) Any given compressive deformation, $\psi(t)$ *with* $\dot{\psi}(t) \leq 0$

b) Any sequence of given $\psi(t)$ *with* $\dot{\psi}(t) \leq 0$ *for* $t \in [t_{2i}, t_{2i+1}]$ *followed by a stress release for* $t \in [t_{2i+1}, t_{2(i+1)})$ *with* $i = 0, ..., n$

c) Any compressive load, $P_{appl}(t) > 0$

Then

$$\Psi_p(t) \geq \psi(t) \qquad\qquad \forall t > 0\,.$$

This proposition allows to get rid of the modulus in (3.13) and rewrite (3.10) and (3.13) as

$$\dot{\Psi}_p(t) = -\frac{1}{3\lambda}\left[\frac{\Psi_p^3(t)-\psi(t)^3}{\psi(t)\Psi_p^2(t)} - \frac{2\tau}{\mu\phi_c}\right]_+ \Psi_p(t)\,, \tag{4.1}$$

$$\dot{\psi}(t) = -\frac{P_{appl}(t)}{3\nu(1-\phi_c)}\psi(t) + \frac{\mu\phi_c}{3\nu(1-\phi_c)}\frac{\Psi_p^3(t)-\psi(t)^3}{\Psi_p^2(t)}\,. \tag{4.2}$$

4.1. Cyclic creep test.

In a cyclic creep test a constant load is applied and the strain induced on the spheroids is measured over a period of time and then the stress on the upper plate is removed. Considering only forces directed along the negative z-axis, it was shown in Proposition 1 (case *c*) that $\Psi_p(t) \geq \psi(t)$ and therefore equations (4.1)-(4.2) hold. Obviously, when the upper plate is lifted-up $P_{appl} = 0$ in equation (4.2).

Equations (4.1) and (4.2) admit non trivial equilibria only if $P_{appl} \leq 2\tau$, as it is stated in the following proposition (proved in the Appendix).

Proposition 2. *In creep tests*

a) if $P_{appl} \leq 2\tau$, then $\Psi_p(t) = 1$ and $\psi(t) \geq \psi_c$: $\dfrac{1}{\psi_c} - \psi_c^2 = \dfrac{P_{appl}}{\mu\phi_c}$ are solutions of equations (4.1) and (4.2), with initial conditions $\Psi_p(0) = 1$ and $\psi(0) = 1$.

b) if $P_{appl}(t) > 2\tau\,,\ \forall t$, then equations (4.1) and (4.2) admit only the trivial equilibrium.

In fact, in the particular case of constant P_{appl}, the right hand side of (4.2) vanishes for non null Ψ_p only if $\dfrac{\Psi_p^3 - \psi^3}{\psi\Psi_p^2} = \dfrac{P_{appl}}{\mu\phi_c}$ that makes the right hand side of (4.1) vanish only if $P_{appl} \leq 2\tau$. As it is evident from plotting the vector field corresponding to (4.1) - (4.2), if $P_{appl} \leq 2\tau$ the solution starting from $\Psi_p(0) = \psi(0) = 1$ will keep $\Psi_p = 1$ while ψ will tend to ψ_c : $\dfrac{1}{\psi_c} - \psi_c^2 = \dfrac{P_{appl}}{\mu\phi_c}$ (see Figure 2, left). On the other hand, if $P_{appl} > 2\tau$, solutions of (4.1)-(4.2) will tend to the trivial equilibria (Figure 2, right).

Hence in a certain range of load, i.e. for $P_{appl} \leq 2\tau$, the cellular aggregate does not undergo an internal reorganization, then $\Psi_p(t) = 1$, whereas $\psi(t)$ decreases until the value ψ_c is reached. In this case, if after some time the load is removed, the specimen will go back to the initial configuration, $\psi_r = 1$, following the classical visco-elastic response, due to the elastic response of cells and the viscous term of the liquid component (see Figure 3).

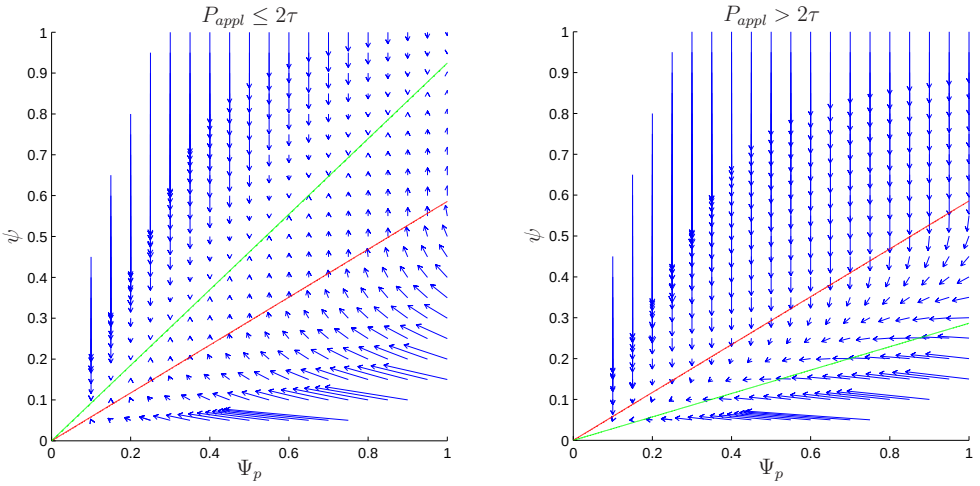

Figure 2: Vector field (blue arrows) corresponding to (4.1) - (4.2), if $P_{appl} \leq 2\tau$ (on the left) and $P_{appl} > 2\tau$ (on the right). The red curve corresponds to $\frac{\Psi_p^3 - \psi^3}{\psi\Psi_p^2} = \frac{2\tau}{\mu\phi_c}$, whereas the green curve to $\frac{\Psi_p^3 - \psi^3}{\psi\Psi_p^2} = \frac{P_{appl}}{\mu\phi_c}$. It is clear that if $P_{appl} \leq 2\tau$, ψ and Ψ will tend to the green curve (in color online). On the other hand if $P_{appl} > 2\tau$, $\Psi_p \to 0$ and $\psi \to 0$.

We observe that if the load is not constant, but smaller than $2\tau \ \forall t$, $\Psi_p(t) = 1$ is still a solution of (4.1).

In order to trigger spheroid internal reorganization P_{appl} must be larger than 2τ, which correspond to the yield condition (3.14). In this case Ψ_p will decrease from $\Psi_p(0) = 1$ according to (4.1), causing a macroscopic remodelling of the multicellular body. Therefore when the upper plate is removed a plastic deformation of the aggregate can be observed. The internal reorganization rate depends on the intensity of the load applied to the aggregate, compared to the yield stress (see Figure 4) and, if $P_{appl}(t) > 2\tau \ \forall t$, it continues until the equilibrium is reached, then $\Psi_p \to 0$ and $\psi \to 0$. This physically means that the aggregate is totally squeezed out between the upper and lower plates of the apparatus.

These results are intuitively reasonable and analytically correct, however they need to be verified with experimental tests, not present in literature. It is important to observe that standard creep tests used for the measurement of mechanical properties of inert material, eventually need to be modified to be suitable for the application to living cell aggregates, that must be kept in healthy conditions during measurements.

4.2. Cyclic deformation test.

In the compression experiments, like those performed in [10, 11, 12], a fixed deformation is applied to cellular spheroids, using a thermostated parallel plate apparatus, immersed in a chamber, filled with pre-warmed tissue culture medium. The specimens used in [10, 11, 12] were obtained from 5 to 6 day old chick embryos, whose cells were dissociated in a solution of trypsin and then placed in a tissue culture medium, to allow them to reorganize. When cultured for about a day, in a

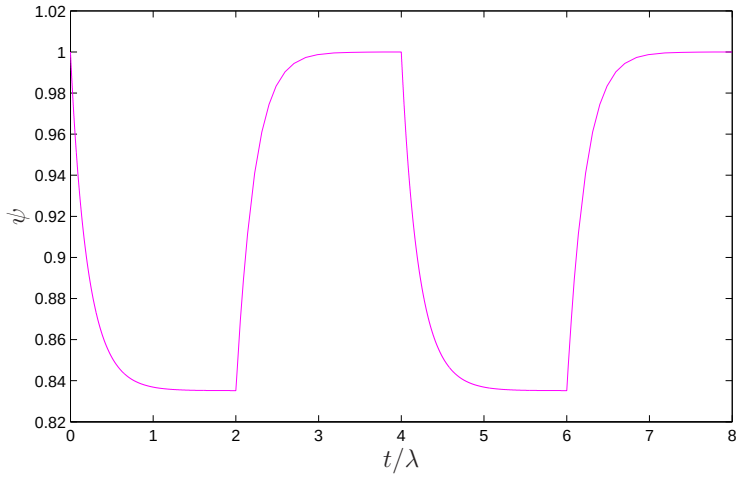

Figure 3: Cycle of compressions when $P_{appl} < 2\tau$ is applied and then removed. The simulation is performed setting the yield stress $\tau = 0.2Pa$ and $P_{appl} = 0.45Pa$, according to the yield condition. The cellular volume ratio, ϕ_c is set equal to 0.8, which is consistent with biological observations [28] and the cell-reorganization time is $\lambda = 22s$. The other parameters can be scaled according to the chosen τ (here: $\mu = 1.1Pa$ and $\nu = 20Pa \cdot s$). The compression and release times are both equal to $2\lambda = 44s$. Being the applied stress under the yield condition, there is no internal reorganization of bonds ($\Psi_p(t) = 1$), therefore when the compression is removed aggregates progressively go back to the initial configuration, $\psi_r = 1$. The liquid component in the mixture is responsible of the delay introduced in the recovery dynamics of spheroids when the upper plate is lifted up.

$37°C$ shaker bath, these multicellular aggregates adopted an almost perfect spherical shape, with a diameter ranging from $200\mu m$ to $500\mu m$.

Recording the force exerted by aggregates upon the upper compression plate, it is possible to observe that living structures undergoing constant deformation, are able to relax the internal stress until an asymptotic value is reached [10, 12].

A variation of this experiment is the cyclic deformation test, like those performed in [10, 11], in which multicellular bodies are forced to periodic compressions at controlled deformation and the compressive force is briefly interrupted at intervals during the approach to shape equilibrium. When compression is interrupted early in this process (as compared to the reorganization time, λ), aggregates can be observed to almost retrieve their initial shape, over the course of a few seconds, whereas after some releases from compressions, a macroscopic deformation can be measured. The process is reiterated until the attainment of an asymptotic behavior, described in the following.

The force relaxation curve and the presence of a plastic deformation are consistent with the visco-elastic model combined with the existence of a yield stress, described in [18], where the experimental stress-relaxation curves are reproduced qualitatively (a direct comparison is not possible due to the lack of some fundamental data). Indeed the internal reorganization (due to the presence of τ), leads to the relaxation of a part of the stress, $P_{appl}(t)$ to the yield value, $P_{appl,\infty} = 2\tau$, regardless of the magnitude of the applied strain ψ_0, as long as ψ_0 satisfies the yield condition stated in (3.14). For such values of ψ_0, if the deformation is released, then the spheroid will not recover its initial shape, because in the meantime the natural configuration has changed. How-

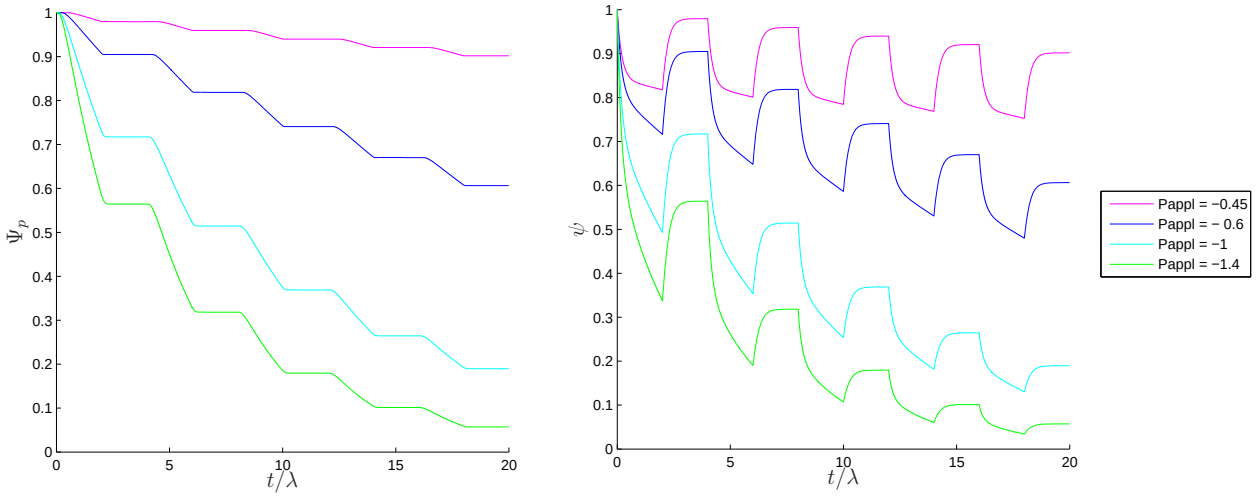

Figure 4: Creep test and release for values of P_{appl} above the yield condition, i.e. $\hat{P} = P_{appl}/\tau > 2$ (with $\tau = 0.2Pa$). The other parameters are the same specified in Figure 3. It is possible to see that, because of the internal reorganization that occurs within the spheroid under compression (Ψ_p dynamics), the natural configuration of the aggregate changes and when the upper plate is removed the multicellular body does not recover its original shape and a macroscopic deformation can be seen. The process that leads to the plastic deformation of aggregates is faster as P_{appl} increases and, independently of P_{appl}, $\Psi_p \to 0$ and $\psi \to 0$, which physically means the rupture of the aggregate.

ever, in [18] this process is instantaneous: if at any instant t_1 the compression is released, then $\Psi_p(t) = \Psi_p(t_1),\ \forall t \geq t_1$ and ψ will suddenly adjust to the value $\psi(t) = \Psi_p(t_1),\ \forall t \geq t_1$ so that $P_{appl} = 0$ (see top curve in Figure 5). This result does not couple well with biological experiments [10, 11, 12], where aggregates progressively expand in height trying to recover their previous shapes, in a process that takes few seconds (e.g. in the specific case of 5-day-old chick embryonic liver cells, 11 s were allowed for this) [10].

The introduction of the viscous component in (2.2), due to the aqueous constituents of aggregates is able to take into account of this phenomenon. To show the behavior of the model described in Section 3 and in order to compare the results obtained with mechanical data in [10], we simulate cycles of compressions at constant deformation.

We know that $\Psi_p(t) \geq \psi(t)$ during the entire process thanks to Proposition 1 (case *b*). Hence during the compression stage, the deformation is imposed and equation (4.1) holds, with $\psi(t) = \psi_0$, whereas when the upper plate is removed, equation (4.1) combined with (4.2) and the condition $P_{appl} = 0$ (stress-free evolution) can describe the shape recovery stage.

The results of the integration of these two systems is plotted in Figure 5, where it is clear that the shape recovery is not instantaneous and its dynamics is controlled by the viscous coefficient: as ν increases the shape recovery will require more time.

Indeed the characteristic time for the shape recovery is given by $\nu/(\mu\phi_c)$. Moreover, the body will not recover the original height, Z, but it presents some plastic deformation. Keeping fixed the mechanical properties of the spheroid, the amplitude of the remodelling and hence the shape

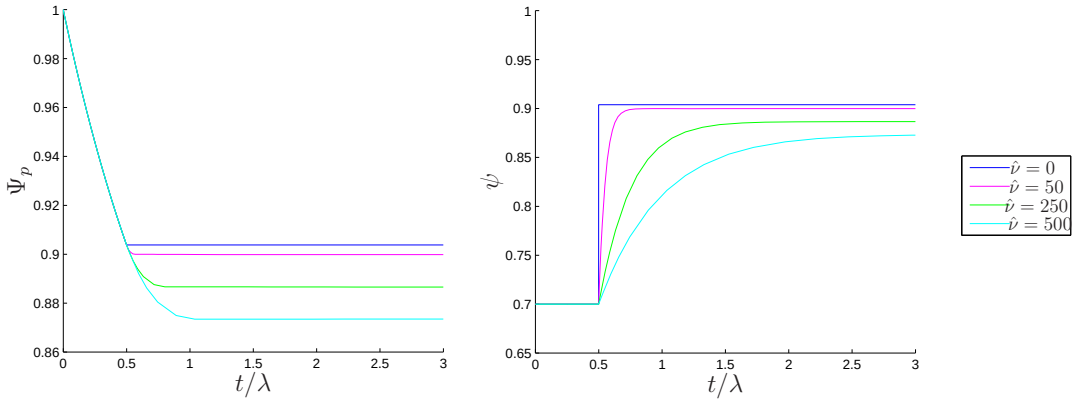

Figure 5: Shape dynamics of cell aggregates when the imposed deformation ($\psi_0 = 0.7$), above the yield value, is released at a given time t_2 (here $t_2 = \lambda/2$, where $\lambda = 22s$). All the simulations are performed with the fixed value of $\tau = 0.2Pa$ and $\phi_c = 0.8$, whereas $\mu = 2.5Pa$. The blue curves represent the model with no viscous effect, $\nu = 0$ corresponding to the model in [18]. It is possible to observe the influence of the viscous parameter, $\hat{\nu} = \nu/\tau$, on the internal reorganization and shape recovery dynamics. According to the experiments in [10] the shape recovery requires tens of seconds, which can be reproduced in our simulations (see magenta curve) setting $\hat{\nu} = 50s$ (i.e. $\nu = 10Pa \cdot s$).

recovery depend on the time under compression. In Figure 6, it is possible to see that in our simulations, with a reorganization time of 22 seconds, a compression of 1 second will be recovered up to 98% while a 10 second compression up to 95%. These results are consistent with biological observations, in fact in Figure 4 of [12] the spheroid aggregate compressed for few seconds almost recovers the original shape, showing a little flattening of the top.

It is also important to remark that even for very long compression times, $t_1 \gg \lambda$, the body will still recover an amount of the deformation, corresponding to the elastic component. Indeed, keeping the compression for times much larger than the reorganization time, spheroids will still experience an elastic recovery that can be considerably smaller (almost 75% in our case, see the leftmost graphs in Figure 6), consistently with Figure 5 of [12]. In other words, aggregates will not keep the imposed deformation, ψ_0 even if the upper plate is removed after a very long time.
It is also interesting to see that during the stress-free evolution of spheroids, the internal reorganization continues following equation (4.1) until an equilibrium is reached, corresponding to the new natural configuration of the remodelled body.

Turning to cycles of compressions at constant deformation and releases, as in [10], a typical result for a twenty-cycle compression/release test is shown in Figure 7. It is possible to see that, at the end of the simulation, the aggregate reaches the maximum of internal reorganization corresponding to the imposed deformation ψ_0 and therefore an asymptotic behavior in the shape recovery is attained. An interesting parameter in the model is μ, which affect the recovery dynamics, along with ν: for small values of this parameter, we have no internal reorganization, because the yield condition (3.14) is not satisfied, and therefore we have no changes in aggregate shapes; on the other hand as μ increases the plastic reorganization of aggregates is more pronounced (see Figure 8).

In [10] measurements are presented in terms of height/width ratio over time under compression.

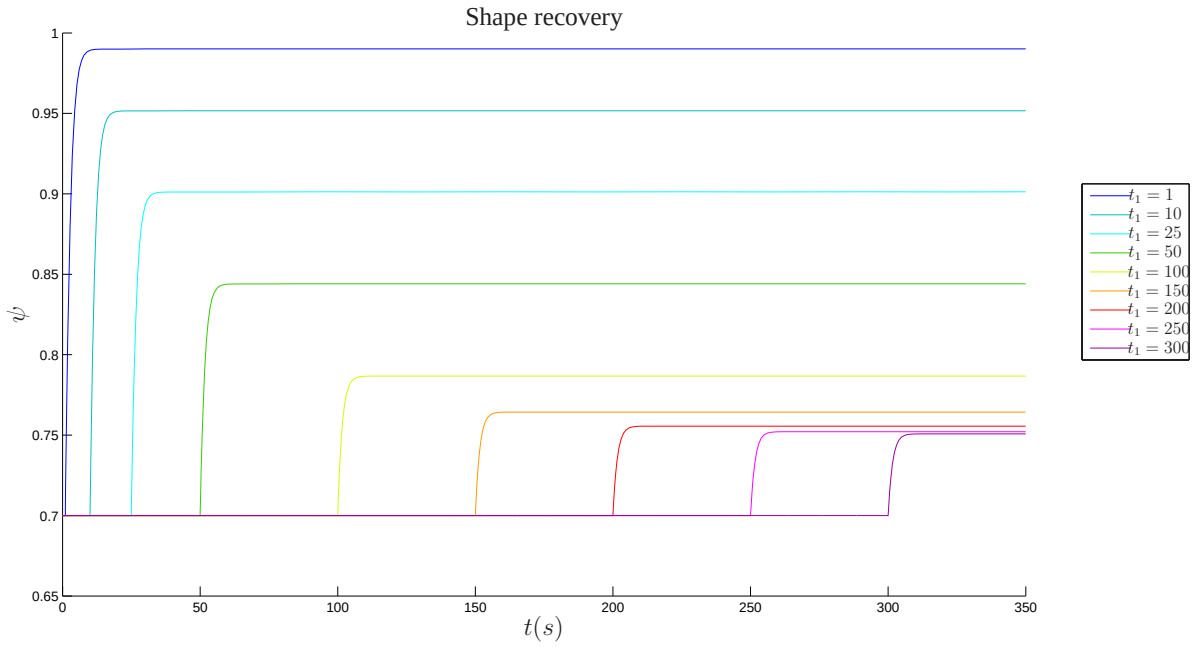

Figure 6: Uniaxial compression test for different values of compression time, t_1 (measured in seconds). The viscosity is chosen in order to reach the shape equilibrium in a period of 11 seconds (i.e. $\nu = 10$, see Figure 5). The shape recovery gets smaller and smaller as the compression time increases, approaching a limit value (in color online).

We try to report the results of our simulations in a similar way, observing that in our model this quantity is represented by $\psi^{3/2}(t)$, from equation (3.1). The results are presented in Figure 9 for different values of the parameter μ and in Figure 10 for different values of reorganization time (keeping μ fixed). The best fit is obtained for a reorganization time equal to $66s$, whereas the best-fitting values of μ depends on the imposed deformation. Indeed it is possible to observe that the equilibrium of (3.10) and (3.13) is reached when $\psi(t) = \Psi_p(t) = \Psi_{p,\infty}$, satisfying the condition indicated in the following proposition (see the appendix for a proof).

Proposition 3. *During the cyclic deformation test at constant deformation, ψ_0, such that the yield condition (3.14) holds, Ψ_p is non increasing, tending to the asymptotic value $\Psi_{p,\infty}$ satisfying*

$$\frac{\Psi_{p,\infty}^3 - \psi_0^3}{\psi_0 \Psi_{p,\infty}^2} = \frac{2\tau}{\mu\phi_c} \tag{4.3}$$

Asymptotically, $\psi(t) \in [\psi_0, \Psi_{p,\infty})$.

The physical interpretation of this result is straightforward. In the stress release process, the deformation gradient between the deformed configuration (where $\psi(t) = \psi_0$) and the final configuration (where $\psi(t) = \psi_\infty$) is

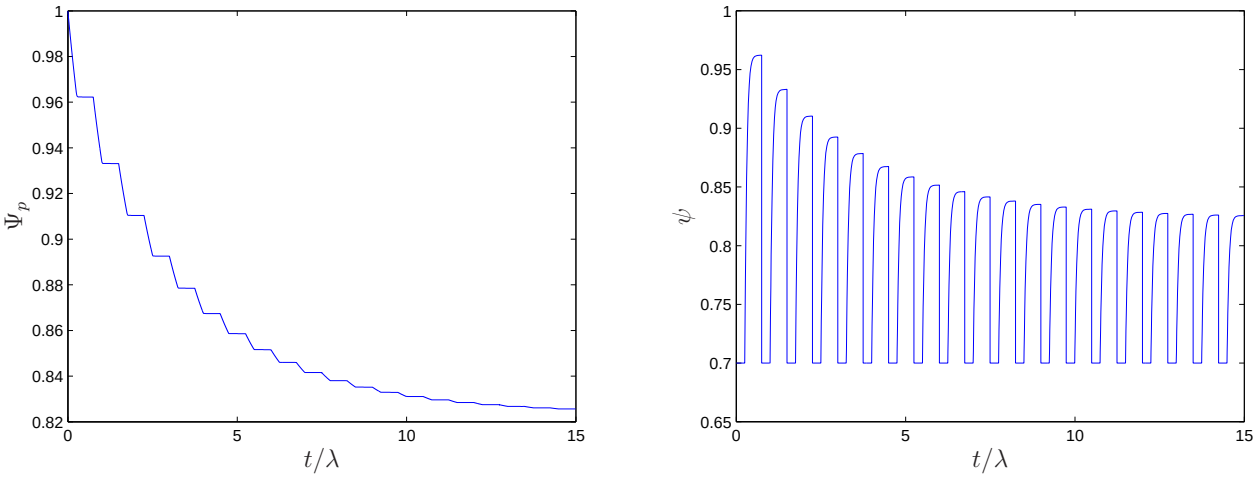

Figure 7: Spheroid behavior under a cycle of 20 compressions at constant deformation and subsequent stress releases. The figures report the internal reorganization Ψ_p (left) and the deformation gradient along the z-axis, ψ (right). The simulation is performed letting the aggregate reorganize under compression for a time $t_c = \lambda/4$ and then remove the upper plate for $11s$ (corresponding to $\lambda/2$).

$$\mathbf{F}_n = \text{diag}\left\{\sqrt{\frac{\psi_0}{\psi_\infty}}, \sqrt{\frac{\psi_0}{\psi_\infty}}, \frac{\psi_\infty}{\psi_0}\right\}$$

then

$$\mathbf{B}_n = \text{diag}\left\{\frac{\psi_0}{\psi_\infty}, \frac{\psi_0}{\psi_\infty}, \frac{\psi_\infty^2}{\psi_0^2}\right\} .$$

If we consider the asymptotic state $\Psi_p = \psi = \Psi_{p,\infty}$ as the reference configuration, a deformation $\dfrac{\psi_0}{\psi_\infty}$ will not trigger further reorganization and the energy is elastically stored, as

$$\phi_c \mathbf{T}_c = \phi_c \left(-(p + \Sigma_c)\mathbf{I} + \mu \mathbf{B}_n\right) = \text{diag}\left\{0, 0, 2\tau\right\} ,$$

where we consider that, when the remodelling inside the spheroid has attained the maximum, the internal stress is equal to 2τ.

We obtain

$$p + \Sigma_c = \mu \frac{\psi_0}{\psi_\infty} , \tag{4.4}$$

$$-\frac{\psi_0}{\psi_\infty} + \frac{\psi_\infty^2}{\psi_0^2} = \frac{2\tau}{\mu \phi_c} . \tag{4.5}$$

Taking into account that $\psi_\infty = \Psi_{p,\infty}$ this is the same result we have obtained only with analytical considerations (see Appendix).

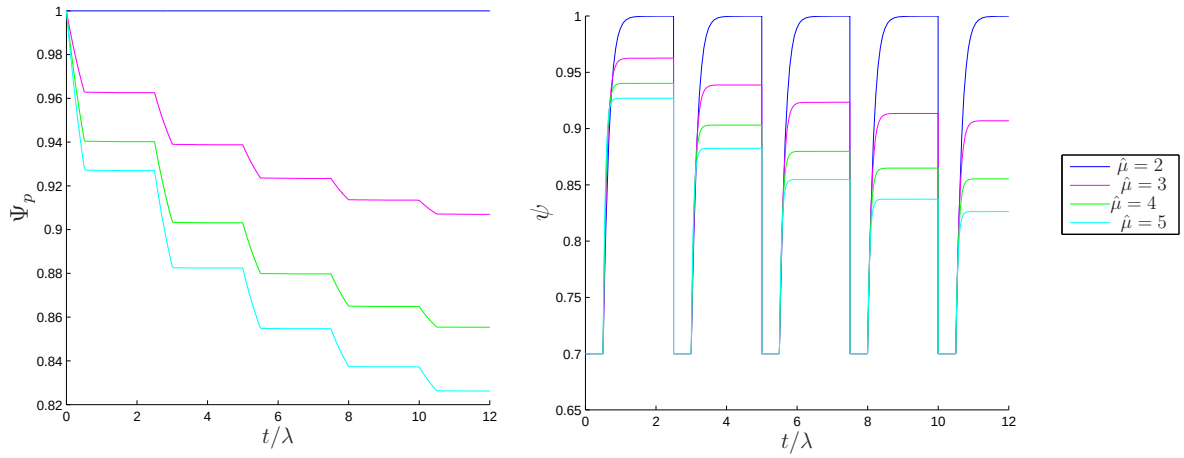

Figure 8: Influence of $\hat{\mu} = \mu\phi_c/\tau$ on spheroid behavior under a compression cycle test ($n = 5$). Aggregates are compressed for $t_c = \lambda/2$ and are let free to expand for $t_r = 2\lambda$ (in order to allow the fulfilment of shape recovery). For the imposed deformation, $\psi_0 = 0.7$, value of $\hat{\mu} < 2.1309$ are not able to induce the internal reorganization of cell, because (3.14) is not satisfied. Therefore $\Psi_p = 1$ (blue curve) and when the compression is released the multicellular body comes back to the original shape in some seconds.

Therefore $\psi_\infty^{3/2}$ is the asymptotic value in Figures 9 and 10, and it is a function of $\psi_0, \tau, \mu, \phi_c$. Thanks to this result, it is possible to find for each ψ_0 a value of μ (see Figure 11), fitting experimental data from [10], where the imposed deformation is unfortunately not known. As shown in figure 11, knowing this datum it would be possible to get the best fitting value of $\mu = \dfrac{mu\phi_c}{\tau}$.

5. Conclusions

The aim of this paper is to study the non-linear mechanical behavior related to the re-organization of multicellular structures. The 3D elasto-visco-plastic model provided here is based on the existence of a yield criterion, above which cells reorganize.
In fact, the cyclic deformation test presented in [10] cannot be described only resorting on a surface tension model, while the model characterized by a yield condition, as that presented here, can.

In this paper we have improved the constitutive model presented in [18], to take into account the viscous component of cell aggregates. Though the constitutive model is kept as simple as possible, we have shown how it can reproduce compression tests performed by [10, 11, 12] and how it can explain creeping phenomena. Moreover with the introduction of the viscous term the model is able to reproduce aggregate release dynamics observed during biological experiments.

Of course, the model can be improved in several directions in order to reproduce more closely the behavior of cell aggregates. An extension can be represented by the inclusion of more cell re-arrangement times, that can be related, for instance, to the detachment of different adhesion proteins inside the cell membrane or to the response occurring inside the cell itself with the rear-

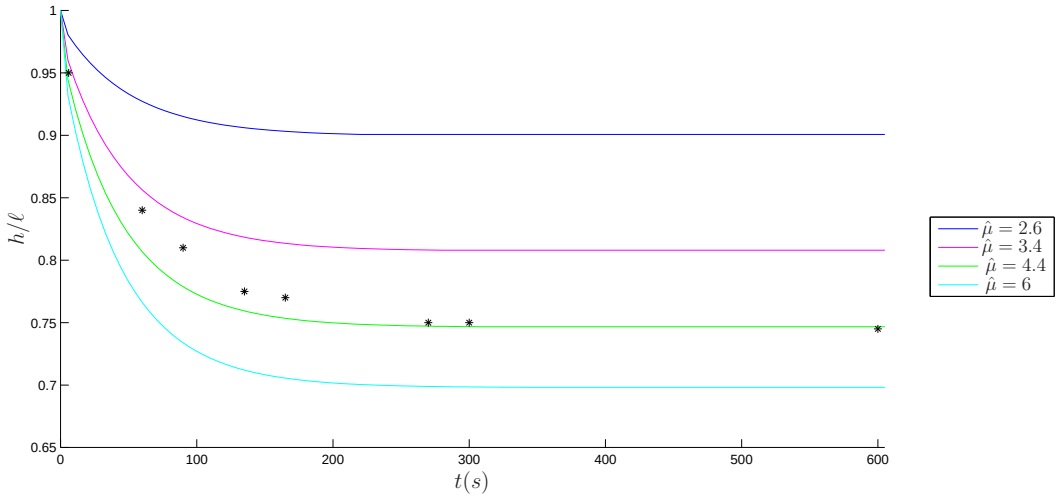

Figure 9: Height/width ratio chart for a cubic multicellular aggregate. The height and width are computed through equation (3.1) and therefore the ratio h/ℓ is represented by the quantity $\psi^{3/2}$ that is plotted for different value of $\hat{\mu} = \mu\phi_c/\tau$, considering the same imposed deformation $\psi_0 = 0.7$ and $\lambda = 50s$. Experimental data obtained by Forgacs et al. [10] are marked with black stars.

rangement of the actin cytoskeleton. The introduction of more relaxation times would certainly lead to a better understanding of the mechanics and a better fit of experimental data. Indeed in the experiments in [10] it is evident the existence of at least two relaxation times in the cellular matter (one of the order of few seconds and the other of the order of tens of seconds).
Furthermore, more realistic 2D and 3D simulations of aggregates deformation have to be performed, in order to obtain a more precise calculation of the height/width ratio, which is of relevant importance for comparing computational data to experimental ones.

At the same time, from the experimental point of view, an important issue is the transposition of biological tests performed on nonphysiological substrates to three-dimensional settings involving complex fibre networks, reproducing the extra-cellular matrix. It is well known that cells are able to remodel their environment extensively, but the interactions between cells and the ECM while under stress remains to be characterized.

Therefore a mathematical model aiming at capturing spheroid nature of porous materials, composed of cells, extracellular materials and liquid, has to be investigated yet, in order to attain a detailed description of soft biological tissue mechanics and understand its implication in some pathologies.

Appendix

Proposition 1. *When the aggregate is compressed according to the following imposed deformation and stress histories:*

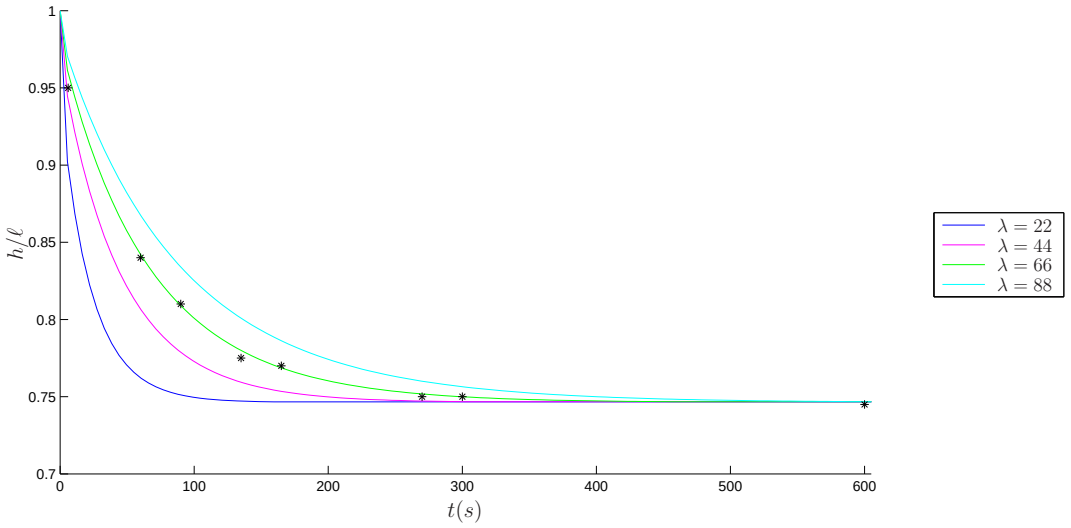

Figure 10: Height/width ratio chart for a cubic multicellular aggregate, for different value of $\lambda(s)$. The parameter μ is fixed, in order to obtain the right asymptotic value (see Figure 9), whereas η changes. The best fit with experimental data (black stars) is obtained for $\lambda = 66\, s$.

a) Any given compressive deformation, $\psi(t)$ with $\dot{\psi}(t) \leq 0$

b) Any sequence of given $\psi(t)$ with $\dot{\psi}(t) \leq 0$ for $t \in [t_{2i}, t_{2i+1}]$ followed by a stress release for $t \in [t_{2i+1}, t_{2(i+1)})$ with $i = 0, ..., n$

c) Any compressive load, $P_{appl}(t) > 0$

Then

$$\Psi_p(t) \geq \psi(t) \qquad\qquad \forall t > 0\,.$$

Proof.

Case a)
We first prove the proposition in the case of a given deformation $\psi(t) < 1$ with $\dot{\psi}(t) \leq 0$ applied to the cellular aggregate for $t \in [0, t_1]$, where t_1 is the time when the upper plate is possibly lifted up. The same proof holds for $t_1 \to \infty$.

Considering that $\Psi_p(0) = 1$, if the imposed deformation $\psi(t)$ is so small that the yield condition (3.14) is not satisfied, from (3.13) the quantity in the square parenthesis is always negative and $\Psi_p(t) = 1 > \psi(t)$.

On the other hand, if the imposed deformation is not so small and the yield condition is overcome, then we can rewrite equation (3.13) regulating the evolution of the internal reorganization, as

$$\dot{\Psi}_p = -\frac{1}{3\lambda}\left[\frac{|\Psi_p^3 - \psi^3|}{\psi\Psi_p^2} - \frac{2\tau}{\mu\phi_c}\right]_+ \text{sgn}(\Psi_p - \psi)\Psi_p\,. \tag{5.1}$$

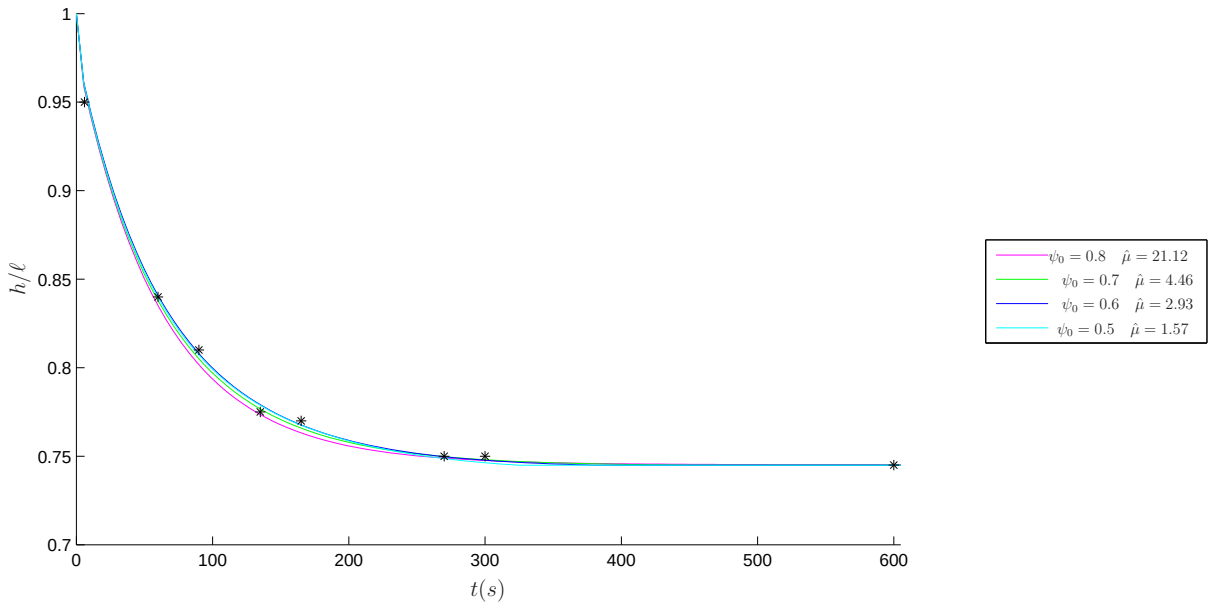

Figure 11: Height/width ratio chart for a cubic multicellular aggregate, for different value of initial deformation ψ_0. To obtain the right fit with experimental data (black stars) [10], μ is computed according to equation (5.12).

It is trivial to check that starting from $\Psi_p(0) = 1$, $\Psi_p(t)$ is always positive. For the thesis, we then define $w(t) = \Psi_p(t) - \psi(t)$ and consider the positive part, w_+, given by

$$w_+(t) = \max\{w(t), 0\} = \begin{cases} w(t) & w(t) > 0 \\ 0 & w(t) \leq 0 \end{cases}$$

and the negative part w_- defined as

$$w_- = \max\{-w(t), 0\} = \begin{cases} -w(t) & w(t) < 0 \\ 0 & w(t) \geq 0 \end{cases}$$

Therefore the function w can be expressed in terms of w_+ and w_-, as $w = w_+ - w_-$.

Then w evolves according to

$$\dot{w} = -\frac{1}{3\lambda}\left[\frac{|\Psi_p^3 - \psi^3|}{\psi\Psi_p^2} - \frac{2\tau}{\mu\phi_c}\right]_+ \text{sgn}(w)\Psi_p - \dot{\psi}\ . \tag{5.2}$$

starting from $w(0) > 0$, since at the initial time $\Psi_p(0) = 1 \geq \psi(0)$.
We multiply each side of (5.2) by w_- and integrate from 0 to an arbitrary time $\tilde{t} \in (0, t_1]$ to get

$$\int_0^{\tilde{t}} \dot{w} w_- dt = -\frac{1}{3\lambda}\int_0^{\tilde{t}} \left[\frac{|\Psi_p^3 - \psi^3|}{\psi\Psi_p^2} - \frac{2\tau}{\mu\phi_c}\right]_+ \text{sgn}(w) w_- \Psi_p dt - \int_0^{\tilde{t}} \dot{\psi} w_- dt =$$
$$= \frac{1}{3\lambda}\int_0^{\tilde{t}} \left[\frac{|\Psi_p^3 - \psi^3|}{\psi\Psi_p^2} - \frac{2\tau}{\mu\phi_c}\right]_+ w_- \Psi_p dt + \int_0^{\tilde{t}} -\dot{\psi} w_- dt \geq 0 \,, \tag{5.3}$$

being both integrands non negative $\forall \tilde{t} \in (0, t_1]$. Hence

$$0 \leq \int_0^{\tilde{t}} \dot{w} w_- dt = -\int_0^{\tilde{t}} \dot{w}_- w_- dt = -\frac{1}{2} w_-^2(\tilde{t}) \leq 0 \,,$$

where we used the condition $w(0) \geq 0$, i.e $w_-(0) = 0$.
Therefore

$$w_-^2(\tilde{t}) = 0 \Longrightarrow w(\tilde{t}) \geq 0 \Longrightarrow \Psi_p(\tilde{t}) \geq \psi(\tilde{t}) \quad \forall \tilde{t} \in (0, t_1] \,.$$

Case b)
If at any time, $t = t_1$, the upper plate is lifted up, then, the equations regulating the evolution of the system, from $t = t_1$ on, are (3.10) and (3.13), that can be rewritten as

$$\dot{\Psi}_p = -\frac{1}{3\lambda}\left[\frac{|\Psi_p^3 - \psi^3|}{\psi\Psi_p^2} - \frac{2\tau}{\mu\phi_c}\right]_+ \text{sgn}(\Psi_p - \psi)\Psi_p \tag{5.4}$$

$$\dot{\psi} = \frac{\mu\phi_c}{3\nu(1-\phi_c)} \frac{\Psi_p^3 - \psi^3}{\Psi_p^2} \,. \tag{5.5}$$

We apply the same method presented before, computing for an arbitrary time $\tilde{t} \in (t_1, t_2]$, where t_2 is the time when the compression is possibly restored (obviously the same proof holds for $t_2 \to \infty$)

$$\int_{t_1}^{\tilde{t}} \dot{w} w_- dt = -\frac{\mu\phi_c}{3\eta}\int_{t_1}^{\tilde{t}} \left[\frac{|\Psi_p^3 - \psi^3|}{\psi\Psi_p^2} - \frac{2\tau}{\mu\phi_c}\right]_+ \text{sgn}(w) w_- \Psi_p dt +$$
$$- \frac{\mu\phi_c}{3\nu(1-\phi_c)}\int_{t_1}^{\tilde{t}} \frac{\Psi_p^2 + \psi\Psi_p + \psi^2}{\Psi_p^2} w w_- dt \,. \tag{5.6}$$

We observe that also in this case, $w_-(t_1) = 0$, being $w(t_1) = \Psi_p(t_1) - \psi(t_1) \geq 0$ (as demonstrated before) and then $\int_{t_1}^{\tilde{t}} \dot{w} w_- dt = -\frac{1}{2} w_-^2$. On the other hand, both terms on the left hand side are always greater or equal to zero, being $\text{sgn}(w) w_- = -w_- \leq 0$ and $w w_- = -w_-^2 \leq 0$.

Then also in this case, we can conclude that

$$w(\tilde{t}) = w_+(\tilde{t}) \geq 0 \Longrightarrow \Psi_p(\tilde{t}) \geq \psi(\tilde{t}) \quad \forall \tilde{t} \in (t_1, t_2] \, .$$

Then it is possible to reiterate the process, together with the one in case *a)* to demonstrate the thesis.

Case c)
In the case of the application of a compressive load, $P_{appl}(t) > 0$, along the negative z-axis

$$\dot{\Psi}_p = -\frac{1}{3\lambda}\left[\frac{|\Psi_p^3 - \psi^3|}{\psi\Psi_p^2} - \frac{2\tau}{\mu\phi_c}\right]_+ \text{sgn}(\Psi_p - \psi)\Psi_p \tag{5.7}$$

$$\dot{\psi} = -\frac{P_{appl}}{3\nu(1-\phi_c)}\psi + \frac{\mu\phi_c}{3\nu(1-\phi_c)}\frac{\Psi_p^3 - \psi^3}{\Psi_p^2} \, . \tag{5.8}$$

Using the same definition for $w(t)$ we have that

$$\begin{aligned}\int_0^{\tilde{t}} \dot{w} w_- dt = & -\frac{\mu\phi_c}{3\eta}\int_0^{\tilde{t}}\left[\frac{|\Psi_p^3 - \psi^3|}{\psi\Psi_p^2} - \frac{2\tau}{\mu\phi_c}\right]_+ \text{sgn}(w) w_- \Psi_p dt + \\ & - \frac{\mu\phi_c}{3\nu(1-\phi_c)}\int_0^{\tilde{t}} \frac{\Psi_p^2 + \psi\Psi_p + \psi^2}{\Psi_p^2} w w_- dt + \\ & + \int_0^{\tilde{t}} \frac{P_{appl}}{3\nu(1-\phi_c)}\psi w_- dt \end{aligned} \tag{5.9}$$

The last integral in equation (5.9) is obviously non negative and therefore also in this case $\Psi_p(t) \geq \psi(t)$.

□

Proposition 2. *In creep tests*

a) if $P_{appl} \leq 2\tau$, then $\Psi_p(t) = 1$ and $\psi(t) \geq \psi_c$: $\dfrac{1}{\psi_c} - \psi_c^2 = \dfrac{P_{appl}}{\mu\phi_c}$ are solutions of equations (4.1) and (4.2), with initial conditions $\Psi_p(0) = 1$ and $\psi(0) = 1$.

b) if $P_{appl} > 2\tau$, then equations (4.1) and (4.2) admit only the trivial equilibrium.

Proof.

Case a)
If $P_{appl}(t) \leq 2\tau \, , \ \forall t$, from equations (4.1)-(4.2), being $\Psi_p(0) = 1$ and $\psi(0) = 1$ the right hand side of (4.1) is initially null, that means $\dot{\Psi}_p(0) = 0$, whereas from (4.2) $\dot{\psi}(0) < 0$.

$\Psi_p = 1$ and $\psi \geq \psi_c$ makes $[\,]_+$ of (4.1) equal to 0. Indeed, being $\dfrac{1}{\psi} - \psi^2$ a decreasing function of ψ,

$$\frac{1}{\psi} - \psi^2 - \frac{2\tau}{\mu\phi_c} \leq \frac{1}{\psi} - \psi^2 - \frac{P_{appl}}{\mu\phi_c} \leq \frac{1}{\psi_c} - \psi_c^2 - \frac{P_{appl}}{\mu\phi_c} = 0\,, \tag{5.10}$$

which holds for all $t \geq 0$.

From (4.2) it is then clear that $\psi = \psi_c$ and $\Psi_p = 1$ makes $\dot{\psi} = 0$ and that $\psi > \psi_c$ and $\Psi_p = 1$ makes $\dot{\psi} < 0$. We will then show that $\psi(t) \geq \psi_c \,\forall t > 0$, using the same argument as in Proposition 1. We define $w = \psi - \psi_c$ and hence

$$\int_0^{\tilde{t}} \dot{w} w_-\, dt \;=\; \frac{\mu\phi_c}{3\nu(1-\phi_c)} \int_0^{\tilde{t}} \left(\frac{1-\psi^3}{\psi} - \frac{P_{appl}}{\mu\phi_c} \right) \psi\, w_-\, dt \geq 0\,, \tag{5.11}$$

where we used the fact that when $w_- \neq 0$, $\psi < \psi_c$ and the parenthesis in the integral is positive.

Therefore

$$0 \leq \int_0^{\tilde{t}} \dot{w} w_-\, dt = -\frac{1}{2} w_-^2(\tilde{t}) \leq 0\,,$$

where we used the condition $w(0) \geq 0$, i.e $w_-(0) = 0$.
For the arbitrariness of $\tilde{t}$, this means that $\psi(t) \geq \psi_c \,\forall t > 0$.

Case b)
The equilibrium for equation (4.1) is reached either if $\Psi_p(t) = 0$ or if the expression in square brackets is negative (i.e. the region above the red line in Figure 2 on the right).

If $P_{appl}(t) > 2\tau$, this second condition corresponding to $\dfrac{\Psi_p^3 - \psi^3}{\psi \Psi_p^2} \leq \dfrac{2\tau}{\mu\phi_c}$, would make the right hand side of (4.2) always strictly negative.
Therefore the only possible equilibrium for (4.1)-(4.2) is $\Psi_{p,\infty} = 0$, $\psi_\infty = 0$

□

Proposition 3. *During the cyclic deformation test at constant deformation, ψ_0, such that the yield condition (3.14) holds, Ψ_p is non increasing, tending to the asymptotic value $\Psi_{p,\infty}$ satisfying*

$$\frac{\Psi_{p,\infty}^3 - \psi_0^3}{\psi_0 \Psi_{p,\infty}^2} = \frac{2\tau}{\mu\phi_c} \tag{5.12}$$

Asymptotically, $\psi(t) \in [\psi_0, \Psi_{p,\infty})$.

Proof. During each compression phase at constant deformation above the yield condition, equation (4.1) states that Ψ_p is non increasing and that $\dot{\Psi}_p = 0$ when $\dfrac{\Psi_{p,\infty} - \psi_0^3}{\psi_0 \Psi_{p,\infty}^2} = \dfrac{2\tau}{\mu\phi_c}$, that corresponds, recalling equation (3.9), to $P_{appl} = 2\tau$.

Considering the system (4.1) and (4.2), with the limit condition $\Psi_p(t_1) = \Psi_{p,\infty}$ and $\psi(t_1) = \psi_0$, we have that $\dot{\Psi}_p(t_1) = 0$ whereas $\dot{\psi}(t_1) > 0$. Actually, being $\psi(t) \leq \Psi_p \ \forall t \geq t_1$ (Proposition 1), $\dot{\psi}(t) > 0$ and then ψ increases until the limit value of $\psi = \Psi_p$ is reached, which corresponds to the equilibrium of (4.2). From the physical point of view this means that the aggregate expands when the compressive force is removed. At the same time, as $\psi(t)$ increases, the ratio $\frac{\Psi_p - \psi^3}{\psi \Psi_p^2}$ decreases, so that square brackets in (4.1) is still equal to zero and therefore $\dot{\Psi}_p(t) = 0 \, \forall t \geq t_1$, then $\Psi_p(t) = \Psi_{p,\infty}$.

Therefore at the equilibrium $\psi_\infty = \Psi_{p,\infty} \ : \ \frac{\Psi_{p,\infty} - \psi_0^3}{\psi_0 \Psi_{p,\infty}^2} = \frac{2\tau}{\mu \phi_c}$.

□

Acknowledgements

The authors wish to thank Andrea Tosin for stimulating discussions. This study was partially funded by the Italian Ministry of University and Research under a grant on "Mathematical Models of the Interactions between cells and environment".

References

[1] D. Ambrosi, F. Mollica. *On the mechanics of a growing tumour.* Int. J. Engng. Sci., 40:1297-1316 (2002).

[2] D. Ambrosi, F. Mollica. *The role of stress in the growth of a multicellular spheroid.* J. Math. Biol., 48:477-499 (2004).

[3] D. Ambrosi, L. Preziosi. *Cell adhesion mechanisms and stress relaxation in the mechanics of tumours.* Biomech. Model. Mechanobiol., 8:397-413 (2009).

[4] D. Ambrosi, K. Garikipati, E. Kuhl. *Mechanics in biology: Cells and tissues*. Phil. Trans. R. Soc. A, 367:3333-3334 (2009).

[5] W. Baumgartner, P. Hinterdorfer, W. Ness, A. Raab, D. Vestweber, H.D.D. Schindler. *Cadherin interaction probed by atomic force microscopy.* Proc. Nat. Acad. Sci. USA, 97:4005-4010 (2000).

[6] C.S. Chen, J. Tan,J. Tien. *Mechanotransduction at cell-matrix and cell-cell contacts.* Annu. Rev. Biomed. Eng., 6:275-302 (2004).

[7] S. Chien, S. Usami, R.J. Dellenback, M. I. Gregersen. *Blood viscosity: Influence of erythrocyte deformation.* Science, 157:827-829 (1967).

[8] S. Chien, S. Usami, R.J. Dellenback, M. I. Gregersen, L. B. Nanninga, M. Mason-Guest. *Blood viscosity: Influence of erythrocyte aggregation.* Science, 157:829-831 (1967).

[9] E. Canetta, A. Duperray, A. Leyrat, C. Verdier. *Measuring cell viscoelastic properties using a force-spectrometer: Influence of the protein-cytoplasm interactions.* Biorheology, 42:298-303 (2005).

[10] G. Forgacs, R.A. Foty, Y. Shafrir, M.S. Steinberg. *Viscoelastic properties of living embryonic tissues: A quantitative study.* Biophys. J., 74:2227-2234 (1998).

[11] R.A. Foty, G. Forgacs, C.M. Pfleger, M.S. Steinberg. *Liquid properties of embryonic tissues: Measurement of interfacial tensions.* Phys. Rev. Lett., 72:2298-2301 (1994).

[12] R.A. Foty, G. Forgacs, C.M. Pfleger, M.S. Steinberg. *Surface tensions of embryonic tissues predict their mutual envelopment behavior.* Development, 122:1611-1620 (1996).

[13] Y.C. Fung. *Microrheology and constitutive equation of soft tissue.* Biorheology, 25:261-270 (1978).

[14] M.E. Gurtin, E. Fried, L. Anand. *The Mechanics and Thermodynamics of Continua*. Cambridge Univ. Pr. (2010).

[15] A. Iordan, A. Duperray, C. Verdier. *Fractal approach to the rheology of concentrated cell suspensions.* Phys. Rev. E, 7:011911 (2008).

[16] M. Lekka, P. Laidler, D. Gil, J. Lekki, Z. Stachura, A.Z. Hrynkiewicz. *Elasticity of normal and cancerous bladder cells studied by scanning force microscopy.* Eur. Biophys. J., 28:312-316 (1999).

[17] M.J. Paszek, N. Zahir, K.R. Johnson, J.N. Lakins, G.I. Rozenberg, A. Gefen, C.A. Reinhart-King, S.S. Margulies, M. Dembo, D. Boettiger, D.A. Hammer, and V. M. Weaver. *Tensional homeostasis and the malignant phenotype.* Cancer Cell, 8:241-254 (2005).

[18] L. Preziosi, D. Ambrosi, C. Verdier. *An elasto-visco-plastic model of cell aggregates*. J. Theor. Biol., 262:35-47 (2010).

[19] L. Preziosi, G. Vitale. *A multiphase model of tumour and tissue growth including cell adhesion and plastic re-organisation.* Math. Mod. Meth. Appl. Sci., in press (2010).

[20] J. Humphrey, K. Rajagopal. *A constrained mixture model for growth and remodeling of soft tissues.* Math. Mod. Meth. Appl. Sci., 22:407-430 (2002).

[21] J. Humphrey, K. Rajagopal. *A constrained mixture model for arterial adaptations to a sustained step change in blood flow.* Biomech. Model. Mechanobiol., 2:109-126 (2003).

[22] E.K. Rodriguez, A. Hoger, A. McCulloch. *Stress-dependent finite growth in soft elastic tissues*. J. Biomech., 27:455-467 (1994).

[23] P. Saramito. *A new constitutive equation for elastoviscoplastic fluid flows.* J. Non-Newtonian Fluid Mech., 145:1-14 (2007).

[24] P. Saramito. *A new elastoviscoplastic model based on the Herschel-Bulkley viscoplasticity.* J. Non-Newtonian Fluid Mech., 158:154-161 (2009).

[25] A.R. Skovoroda, A.N. Klishko, D.A. Gusakyan, Y.I. Mayevskii, V.D. Yermilova, G.A. Oranskaya, A.P. Sarvazyan. *Quantitative analysis of the mechanical characteristics of pathologically changed soft biological tissues.* Biophysics, 40:1359-1995 (1995).

[26] M. Sun, J. Graham, B. Hegedus, F. Marga, Y. Zhang, G. Forgacs, M. Grandbois. *Multiple membrane tethers probed by atomic force microscopy.* Biophys. J., 89:4320-4329 (2005).

[27] L.A. Taber, J.D. Humphrey. *Stress-modulated growth, residual stress, and vascular heterogeneity*. J. Biomech. Eng., 123:528-535 (2001).

[28] G. A. Truskey, F. Yuan, D.F. Katz. *Transport phenomena in biological systems.* Prentice Hall (2009)

[29] A. Vaziri, A. Gopinath. *Cell and biomolecular mechanics in silico*. Nat. Materials, 7:15-23 (2008).

[30] C. Verdier. *Review. Rheological properties of living materials: From cells to tissues.* J. Theor. Medicine, 5:67-91 (2003).

[31] C. Verdier, J. Etienne, A. Duperray, L. Preziosi. *Review: Rheological properties of biological materials*. C. R. Phys., 10:790-811 (2009).

[32] B.S. Winters, S.R. Shepard, R.A. Foty. *Biophysical measurement of brain tumor cohesion.* Int. J. Cancer, 114:371-379 (2005).